Colorimetric Sensor Arrays for Volatile Organic Compounds

Michael C. Janzen,[†] Jennifer B. Ponder,[†] Daniel P. Bailey, Crystal K. Ingison, and Kenneth S. Suslick*

Department of Chemistry, University of Illinois at Urbana−Champaign, 600 South Mathews Avenue, Urbana, Illinois 61801

The development of a low-cost, sensitive colorimetric sensor array for the detection and identification of volatile organic compounds (VOCs) is reported. Using an array composed of chemoresponsive dyes, enormous discriminatory power is possible in a simple device that can be imaged easily with an ordinary flatbed scanner. Excellent differentiation of closely related organic compounds can be achieved, and a library of 100 VOCs is presented. The array discriminates among VOCs by probing a wide range of intermolecular interactions, including Lewis acid/base, Brønsted acid/base, metal ion coordination, hydrogen bonding, and dipolar interactions. Importantly, by proper choice of dyes and substrate, the array is essentially nonresponsive to changes in humidity.

Array-based vapor sensing has emerged as a potentially powerful approach toward the detection of chemically diverse analytes. Based on cross-responsive sensor elements, rather than specific receptors for specific analytes, these systems produce composite responses unique to an odorant in a fashion similar to the mammalian olfactory system.[1] In this design architecture, one receptor responds to many analytes and many receptors respond to any given analyte. A distinct pattern of responses produced by the array provides at least the possibility of a characteristic fingerprint for each analyte. In this paper, we provide a detailed account of the ability of our colorimetric sensor arrays to distinguish among a large family of volatile organic compounds (VOCs); earlier communications have provided related, but much more limited, data and analysis.[2] Our primary purpose here is to discuss selectivity; issues of sensitivity will be discussed separately in future reports.

Previous array technologies for such electronic noses generally rely on multiple, cross-reactive sensors based primarily on changes in properties (e.g., mass, volume, conductivity) of some set of polymers or on electrochemical oxidations at a set of heated metal oxides. Specific examples include conductive polymers and polymer composites,[3] polymers impregnated with a solvatochromic dye or fluorophore,[4] mixed metal oxide sensors,[5] and polymer-coated surface acoustic wave devices.[6] In these reports, it naively appears that a high level of sensor diversity has been examined with each approach; on closer examination, however, this proves not to be the case and the interactions of such sensors with analytes are nearly always limited to the weakest and least specific of intermolecular interactions, primarily van der Waals and physical adsorption interactions between sensor and analyte. We believe this to be a fundamental flaw in the development of

---

* Corresponding author: (tel) 1-217-333-2794; (fax) 1-217-333-2685; (e-mail) ksuslick@uiuc.edu.

[†] Contributed equally to this work.

(1) (a) Stetter, J. R., Pensrose, W. R., Eds. *Artificial Chemical Sensing: Olfaction and the Electronic Nose*; Electrochemical Society: Pennington, NJ, 2001. (b) Gardner, J. W.; Bartlett, P. N. *Electronic Noses: Principles and Applications;* Oxford University Press: New York, 1999. (c) Persuad, K.; Dodd, G. H. *Nature* **1982,** *299,* 352. (d) Albert, K. J.; Lewis, N. S.; Schauer, C. L.; Sotzing, G. A.; Stützel, G. A.; Stitzel, S. E.; Vaid, T. P.; Walt, D. R. *Chem. Rev.* **2000,** *100,* 2595−2626. (e) Lewis, N. S. *Acc. Chem. Res.* **2004,** *37,* 663−672. (f) James, D.; Scott, S. M.; Ali, Z.; O'Hare, W. T. *Microchim. Acta* **2005,** *149,* 1−17. (g) Walt, D. R. *Anal. Chem.* **2005,** *77,* 45A.

(2) (a) Rakow, N. A.; Suslick, K. S. *Nature* **2000,** *406,* 710−713. (b) Suslick, K. S.; Rakow, N. A. *Artificial Chemical Sensing: Olfaction and the Electronic Nose*; Stetter, J. R., Penrose, W. R., Eds.; Electrochemical Society: Pennington, NJ: 2001; pp 8−14. (c) Suslick, K. S.; Rakow, N. A.; Sen, A. *Tetrahedron* **2004,** *60,* 11133−11138. (d) Suslick, K. S. *MRS Bull.* **2004,** *29,* 720−725. (e) Rakow, N. A.; Sen, A.; Janzen, M. C.; Ponder, J. B.; Suslick, K. S. *Angew. Chem., Int. Ed.* **2005,** *44,* 4528−4532. (f) Zhang, C.; Suslick, K. S. *J. Am. Chem. Soc.* **2005,** *127,* 11548−11549.

(3) (a) Gallazzi, M. C.; Tassoni, L.; Bertarellli, C.; Pioggia, G.; Di Francesco, F.; Montoneri, E. *Sens. Actuators, B* **2003,** *88,* 178−189. (b) Guadarrana, A.; Rodriquez-Mendez, M. L.; de Saja, J. A. *Anal. Chim. Acta* **2002,** *455,* 41−47. (c) Garcia-Guzman, J.; Ulivieri, N.; Cole, M.; Gardner, J. W. *Sens. Actuators, B* **2003,** *95,* 232−243 (d) Burl, M. C.; Doleman, B. J.; Schaffer, A.; Lewis, N. S. *Sens. Actuators, B* **2001,** *72,* 149−159. (e) Wang, Y.; Sotzing, G. A.; Weiss, R. A. *Chem. Mater.* **2003,** *15,* 375−377. (f) Hopkins, A. R.; Lewis, N. S. *Anal. Chem.* **2001,** *73,* 884−892. (g) Feller, J. F.; Grohens, Y. *Sens. Actuators, B* **2004,** *97,* 231−242. (h) Ferreira, M.; Riul, A., Jr.; Wohnrath, K.; Fonseca, F. J.; Oliveira, O. N., Jr.; Mattoso, L. H. C. *Anal. Chem.* **2003,** *75,* 953−955. (i) Riul, A., Jr.; de Sousa, H. C.; Malmegrim, R. R.; dos Santos, D. S., Jr.; Carvalho, A. C. P. L. F.; Fonseca, F. J.; Oliveira, O. N., Jr.; Mattoso, L. H. C. *Sens. Actuators, B* **2004,** *98,* 77−82. (j) Sotzing, G. A.; Briglin, S. M.; Grubbs, R. H.; Lewis, N. S. *Anal. Chem.* **2000,** *72,* 3181−3190. (k) Segal, E.; Tchoudakov, R.; Narkis, M.; Siegmann, A.; Wei, Y. *Sens. Actuators, B* **2005,** *104,* 140−150. (l) Burl, M. C.; Sisk, B. C.; Vaid, T. P.; Lewis, N. S. *Sens. Actuators, B* **2002,** *87,* 130−149. (m) Severin, E. J.; Doleman, B. J.; Lewis, N. S. *Anal. Chem.* **2000,** *72,* 658−668. (n) Freund, M. S.; Lewis, N. S. *Proc. Natl. Acad. Sci. U.S.A.* **1995,** *92,* 2652−2656. (o) Gardner, J. W.; Pike, A.; Derooij, N. F.; Koudelkahep, M.; Clerc, P. A.; Hierlemann, A.; Gopel, W. *Sens. Actuators, B* **1995,** *26,* 135−139. (p) Bartlett, P. N.; Archer, P. B. M.; Ling-Chung, S. K. *Sens. Actuators, B* **1989,** *19,* 125−140. (q) Shurmer, H. V.; Gardner, J. W.; Corcorran, P. *Sens. Actuators, B* **1990,** *1,* 256−260. (r) Lonergan, M. C.; Severin, E. J.; Doleman, B. J.; Beaber, S. A.; Grubbs, R. H. *Chem. Mater.* **1996,** *8,* 2298−2312.

(4) (a) Chen, S.-J.; Chang, H.-T. *Anal. Chem.* **2004** *76,* 3727−3734. (b) Hsieh, M.-D.; Zellers, E. T. *Anal. Chem.* **2004,** *76,* 1885−1895. (c) Li, D.; Mills, C. A.; Cooper, J. M. *Sens. Actuators, B* **2003,** *92,* 73−80. (d) Albert, K. J.; Walt, D. R. *Anal. Chem.* **2003,** *75,* 4161−4167. (e) Epstein, J. R.; Lee, M.; Walt, D. R. *Anal. Chem.* **2002,** *74,* 1836−1840. (f) Albert, K. J.; Walt, D. R.; Gill, D. S.; Pearce, T. C. *Anal. Chem.* **2001,** *73,* 2501−2508. (g) Stitzel, S. E.; Cowen, L. J.; Albert, K. J.; Walt, D. R. *Anal. Chem.* **2001,** *73,* 5266−5271. (h) Albert, K. J.; Walt, D. R. *Anal. Chem.* **2000,** *72,* 1947−1955. (i) Dickinson, T. A.; White, J.; Kauer, J. S.; Walt, D. R. *Nature* **1996,** *382,* 697−700. (j) Dickinson, T. A.; Michael, K. L.; Kauer, J. S.; Walt, D. R. *Anal. Chem.* **1996,** *68,* 2192−2198. (k) Dickinson, T. A.; Michael, K. M.; Kauer, J. S.; Walt, D. R. *Anal. Chem.* **1999,** *71,* 2192−2198.
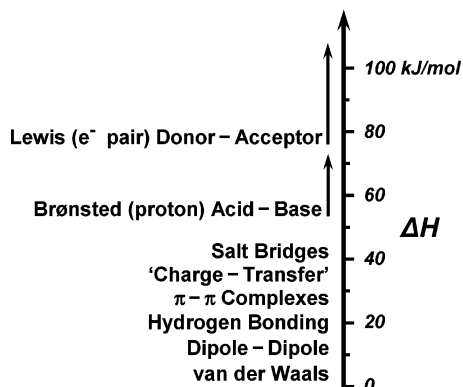

Figure 1. Intermolecular interactions on a semiquantitative energy scale.

chemical sensors with both high sensitivity and high selectivity. Despite some successes with prior electronic nose systems, the limited range of sensor−analyte interactions limits both their sensitivity for detection of compounds at low concentrations relative to their vapor pressures and their selectivity for discrimination between compounds; the latter proves especially problematic in interference from the large environmental changes in humidity.

Design of a Colorimetric Sensor Array. The detection and identification of chemicals fundamentally is supramolecular chemistry and intrinsically relies on the interactions between molecules and atoms. The classification of intermolecular interactions is well established (Figure 1) and involves bond formation and coordination, acid−base interactions, hydrogen-bonding, charge-transfer and $\pi-\pi$ molecular complexation, dipolar and multipolar interactions, and van der Waals interaction and physical adsorption. The use of an array of sensors that probes this full range of intermolecular interactions is essential to the further development of array technology.

In addition, the development of new sensor technology faces the dilemma of trying to create sensors that are *both* increasingly sensitive and increasingly robust (i.e., stable to exposure to analytes or the environment). Beyond a certain point, the more sensitive a sensor becomes, inherently the less robust it can be. The path around this dilemma is the development of disposable sensors, which are *not* integrated to the readout device, thus unlinking the opposing demands.

A final consideration is the practical issues of cost and portability. We would argue that few technologies are as advanced or as inexpensive as visual imaging (e.g., digital cameras and scanners). This reflects, of course, our own species' visual orientation.

In merging these three considerations, we have previously reported a general approach to an "optoelectronic nose" based on the colorimetric array detection using a chemically diverse range of chemically responsive dyes.[2,7] Fundamentally, we convert olfactory-like responses to a visual output. In many ways, our colorimetric sensor array revisits the earlier, pre-electronic era of analytical chemistry,[8] updated by the addition of modern digital imaging and pattern recognition techniques. Here we present extensions of our colorimetric sensor array and explore its application to the determination of chemical vapors.

The design of an expanded colorimetric sensor array is based on two fundamental requirements: (1) each chemically responsive dye must contain a center to interact strongly with analytes, and (2) each interaction center must be strongly coupled to an intense chromophore. The first requirement implies that the interaction must not be simply physical adsorption, but rather must involve other, stronger chemical interactions. Chemoresponsive dyes are those dyes that change color, in either reflected or absorbed light, upon changes in their chemical environment. The consequent dye classes from these requirements are (1) Lewis acid/base dyes (i.e., metal ion-containing dyes), (2) Brønsted acidic or basic dyes (i.e., pH indicators), and (3) dyes with large permanent dipoles (i.e., zwitterionic solvatochromic dyes) (Figure 2). The importance of strong sensor−analyte interactions is highlighted by recent indications that the mammalian olfactory receptors are, in many cases, metalloproteins and that odorant ligation to the metal center is intrinsic to the mechanism of action.[9]

EXPERIMENTAL SECTION

Colorimetric sensor arrays are commercially available from ChemSensing, Inc., Northbrook, Illinois (www.chemsensing.com), part number CSI.031. The VOC analytes used in this study were reagent grade and were used as received, except for alkenes, each of which was passed through an alumina column.

For all sensing experiments, each sensor array was held in a glass and Teflon cell with the array imaged through optical glass by an Epson Perfection 1670 flatbed scanner to acquire the "before" image. Above the array, a piece of filter paper was suspended without contact. An analyte was then placed on the filter paper (5−20 μL for a liquid sample or 300 mg for a solid

(5) (a) Gardner, J. W.; Bartlett, P. N. *Sensors and Sensory Systems for an Electronic Nose*; Kluwer Academic Publishers: Dordrecht, 1992. (b) Zampolli, S.; Elmi, I.; Ahmed, F.; Passini, M.; Cardinali, G. C.; Nicoletti, S.; Dori, L. *Sens. Actuators, B* **2004**, *101*, 39−46. (c) Tomchenko, A. A.; Harmer, G. P.; Marquis, B. T.; Allen, J. W. *Sens. Actuators, B* **2003**, *93*, 126−134. (d) Nicolas, J.; Romain, A.-C. *Sens Actuators, B* **2004**, *99*, 384−392. (e) Marquis, B. T.; Vetelino, J. F. *Sens. Actuators, B* **2001**, *77*, 100−110. (f) Ehrmann, S.; Jüngst, J.; Goschnick, J.; Everhard, D. *Sens. Actuators, B* **2000**, *65*, 247−249. (g) Getino, J.; Arés, L.; Robla, J. I.; Horrillo, M. C.; Sayago, I.; Fernández, M. J.; Rodrigo, J.; Gutiérrez, J. *Sens. Actuators, B* **1999**, *59*, 249−254. (h) Heilig, A.; Bârsan, N.; Weimar, U.; Schweizer-Berberich, M.; Gardner, J. W.; Göpel, W. *Sens. Actuators, B* **1997**, *43*, 45−51. (i) Gardner, J. W.; Shurmer, H. V.; Corcoran, P. *Sens. Actuators, B* **1991**, *4*, 117−121 (j) Gardner, J. W.; Shurmer, H. V.; Tan, T. T. *Sens. Actuators, B* **1992**, *6*, 71−75. (k) Corcoran, P.; Shurmer, H. V.; Gardner, J. W. *Sens. Actuators, B* **1993**, *15*, 32−37. (l) Gardner, J. W.; Pike, A.; de Rooji, N. F.; Koudelka-Hep, M.; Clerc, P. A.; Hierlemann, A.; Göpel, W. *Sens. Actuators, B* **1995**, *26*, 135−139.

(6) (a) Grate, J. W. *Chem. Rev.* **2000**, *100*, 2627−2648. (b) Hsieh, M.-D.; Zellers, E. T. *Anal. Chem.* **2004**, *76*, 1885−1895. (c) Grate, J. W.; Wise, B. M.; Gallagher, N. B. *Anal. Chim. Acta* **2003**, *490*, 169−184. (d) Penza, M.; Cassano, G. *Sens. Actuators, B* **2003**, *89*, 269−284. (e) Levit, N.; Pestov, D.; Tepper, G. *Sens. Actutors, B* **2002**, *82*, 241−249. (f) Grate, J. W.; Patrash, S. J.; Kaganove, S. N.; Abraham, M. H.; Wise, B. M.; Gallagher, N. B. *Anal. Chem.* **2001**, *73*, 5247−5259. (g) Hierlemann, A.; Zellers, E. T.; Ricco, A. J. *Anal. Chem.* **2001**, *73*, 3458−3466. (h) Grate, J. W.; Zellers, E. T. *Anal. Chem.* **2000**, *72*, 2861−2868. (i) Ballantine, D. S., Jr.; Rose, S. L.; Grate, J. W.; Wohltjen, H. *Anal. Chem.* **1986**, *58*, 3058−3066. (j) Rose-Pehrsson, S. L.; Grate, J. W.; Ballantine, D. S., Jr.; Jurs, P. C. *Anal. Chem.* **1988**, *60*, 2801−2811. (k) Patrash, S. J.; Zellers, E. T. *Anal. Chem.* **1993**, *65*, 2055−2066.

(7) (a) Suslick, K. S.; Rakow, N. A. U.S. Patent 6,368,558, April 9, 2002. (b) Suslick, K. S.; Rakow, N. A. U.S. Patent 6,495,102, December 17, 2002.

(8) Kolthoff, I. M. *Acid Base Indicators*; Rosenblum, C., trans.; Macmillan: New York, 1937.

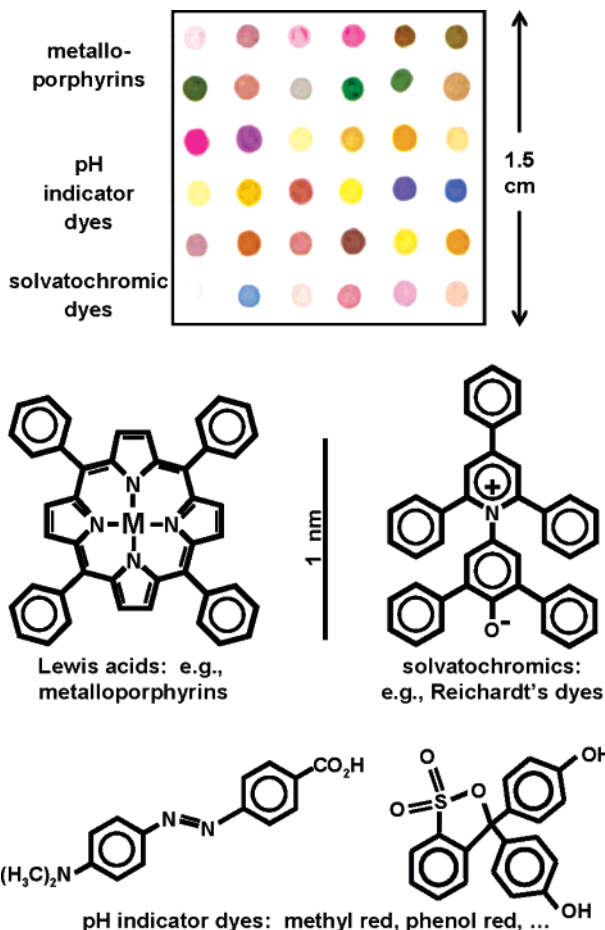(9) Wang, J.; Luthey-Schulten, Z.; Suslick, K. S. *Proc. Natl. Acad. Sci. U.S.A.* **2003**, *100*, 3035−3039.

Figure 2. Disposable colorimetric sensor array, its dye classes, and some representative examples drawn to scale.[2]

Figure 3. Image of the 36-dye colorimetric sensor array before exposure (left) and after exposure to decylamine (middle) after equilibration at full vapor pressure at 295 K. A subtraction of the two images yields a difference vector in 108 dimensions (i.e., 36 changes in red, green, and blue color values, each ranging from a minimum of −510 to +510); this vector is usefully visualized using a difference map (right), which shows the absolute values of the color changes. For purposes of display to increase the color palate, the color range of the difference map has been expanded from 6 to 8 bits per color (i.e., an RGB range of 4−67 is shown expanded to 0−255).

Chemometric analysis on the difference vectors was carried out using Multi-Variate Statistical Package (v. 3.1, Kovach Computing).

RESULTS AND DISCUSSION

Sensor Array. As discussed earlier, the required dye classes for an optoelectronic sensor array include (1) Lewis acid/base dyes (i.e., metal ion-containing dyes), (2) Brønsted acidic or basic dyes (i.e., pH indicators), and (3) dyes with large permanent dipoles (i.e., zwitterionic solvatochromic dyes) (Figure 2). For recognition of analytes with Lewis acid/base capabilities, the use of porphyrins and their metal complexes is a natural choice. Metalloporphyrins are nearly ideal for the detection of metal-ligating vapors because of their open coordination sites for axial ligation, their large spectral shifts upon ligand binding, their intense coloration, and their ability to provide ligand differentiation based on metal-selective coordination. Importantly, they are cross-responsive dyes, showing responses to a large variety of different analytes to different degrees and by different color changes. Common pH indicator dyes change color in response to changes in the proton (Brønsted) acidity or basicity of their environment. Solvatochromic dyes change color in response to changes in the general polarity of their environment, primarily through strong dipole−dipole and dispersion interactions. To some extent, all dyes inherently are solvatochromic, although obviously some are more responsive than others.

The interference of atmospheric humidity on sensor performance is a serious problem with previous electronic nose technology. The high concentration of water vapor in the environment and (even more importantly) its large and changeable range make the accurate detection of volatile compounds at low concentration exceptionally challenging. Water vapor ranges in the environment from <2000 to >20 000 ppmv; if one is interested in few ppmv, and even few ppb, concentrations of VOCs, even a very low level of interference from water is therefore intolerable. Physisorption of molecules on surfaces is dominated by the relative hydrophobicity of the adsorbate and adsorbent. It should be no surprise, therefore, that a very serious weakness in prior electronic nose technology is sensitivity to changes in humidity.

Because the colorimetric sensors in the array have been selected from hydrophobic, water-insoluble dyes and have been contact printed as nonaqueous, hydrophobic solutions onto

sample) and the cell was sealed; because excess liquid or solid analyte has been added to the sealed cell, at equilibrium the cell is saturated with the full vapor pressure of the analyte at room temperature. A total of 100 VOCs were exposed to arrays at 295 K; triplicate arrays were used for each analyte to test the reproducibility of the array response. The "after" images are then acquired after equilibration (equilibration determined by repeated scans at longer times). Response time is mass transport limited in these experiments. In flow systems at 500 mL/min, equilibration of the arrays is complete in 2 min even at 1 ppmv analyte concentration. Difference maps are obtained by taking the difference of the red, green, and blue (RGB) values from the center of every dye spot (∼300 pixels) from the "before" and "after" images. Averaging of the centers of the spots avoids artifacts from nonuniformity of the dye spots, especially at their edges. Subtraction of the two images yields a difference vector of $3N$ dimensions where N is total number of spots; for our six by six array, this difference vector is 108 dimensions (i.e., 36 changes in red, green, and blue color values), each dimension ranging from −510 to +510). The difference vectors are provided in the Supporting Information. These subtractions can be done with Photoshop or with a customized software package, ChemEye (ChemSensing, Inc.). The difference vector is conveniently visualized as a map of the absolute values of the color changes of the after minus the before images of the same array of dyes (as shown in Figure 3).
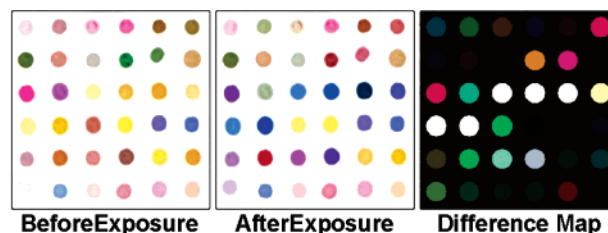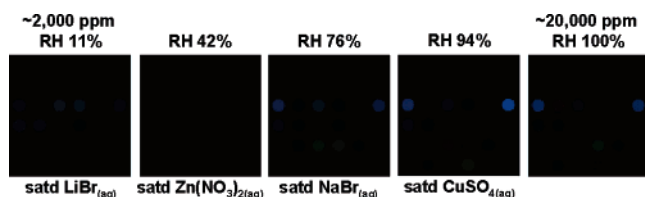
Figure 4. Difference map of saturated aqueous salt solutions at 295 K shown with the color range expanded from 6 to 8 bits per color (RGB range of 4−67 expanded to 0−255). The array is essentially nonresponsive to changes in RH.

hydrophobic substrates, these arrays are essentially impervious to changes in relative humidity (RH), as seen in Figure 4. The arrays were exposed to water vapor from pure water (RH 100%) and from saturated salt solutions whose water vapor pressures ranged from 11 to 94% RH:[10] the dyes in the sensor array (Figure 4) are unresponsive to water vapor. Similarly, the response to other analytes is not affected by the presence or absence of RH over this range. In fact, it is possible to use similar arrays directly in water for the sensing of dilute aqueous solutions of organic compounds.[2f]

Discrimination of VOCs. To demonstrate the ability of the sensor array to discriminate among analytes, 100 different volatile organic compounds (Table 1) were tested representing common organic functionalities including primary, secondary, tertiary, and aromatic substituents of amines, arenes, alcohols, aldehydes, carboxylic acids, esters, hydrocarbons, ketones, phosphines, and thiols. Experiments were run until full equilibration was demonstrated by comparison of repeated scans. The response of the array is mass transport limited; interaction times (ligation, proton transfer, etc.) are much faster than the typically observed array response. Under proper conditions of rapid gas flow, equilibration of the array occurs within 2 min, even at ppmv analyte concentrations; under static diffusion conditions, equilibration (especially with low volatility analytes) can take 1 h or more, depending of course on the specific cell configuration.

Every spot in the array is uniquely described by RGB color values; for an eight-bit color scanner, this spans the range of 0−255: i.e., black is (0, 0, 0) and white is (255, 255, 255). It is convenient to represent the array response to any analyte, odorant, or mixture as the difference between each spot's initial RGB values and those after exposure. Thus, every analyte response is represented digitally by a 108-dimensional vector (i.e., 36 red, green, and blue color difference values). A color difference map is useful for visualization of these data and is easily generated by taking the absolute value of the difference of RGB values between the "before" and "after" image (Figure 3). These difference maps are usually not displayed over the full 0−255 range, since RGB changes rarely span the entire 256 range; rather, for improved display, the color palette of the difference map is enhanced by expanding the displayed color range of 4−67 (i.e., six bit color) to 0−255 (i.e., eight bit color). In this example, any change in RGB values that is less than 4 is treated as background noise and the difference is set zero; for any change between 4 and 67, the RGB value is prorated into the full 256 RGB range; for RGB changes greater than 67, the difference goes to 255. All data

analysis, however, relies strictly on the original digital differences in the RGB values that make up the 108-dimensional vector and are in no way affected by the difference map display parameters; the complete digital data of the full database are available in the Supporting Information.

Representative difference maps for 48 of the total 100 organic compounds in the database are shown in Figures 5 and 6. Excellent discrimination among a very wide range is observed even without any statistical or chemometric analysis. The difference maps highlight the ability of the array to discriminate among all common organic functional groups. Closely related compounds from the different chemical classes are easily differentiated: the color patterns of compounds within a class (e.g., amines vs acids vs aldehydes, etc.) are very different from each other class and easily distinguishable without any chemometric manipulation. In addition, the difference maps of individual compounds are unique and distinct by eye, even by comparison to very similar compounds in the same class. The weaker responding analytes (thiols, esters, alcohols, hydrocarbons) are displayed in Figure 6 with an expanded color range (i.e., RGB values of 8−17 expanded to 0−255), and even here with weakly coordinating analytes, analyte discrimination can be achieved easily.

Sensitivity. We have not tried in this work to determine the limits of detection (LODs) or of recognition (LORs) for our colorimetric sensor array, focusing instead on analyte identification and selectivity. LODs for prior electronic noses have generally been well above the ppmv level, but gas concentrations in ppmv can be deceptive. It is well recognized that the thermodynamic chemical potential of vapors, which determines the on−off equilibrium for analyte binding to polymer or metal oxide sensors, is best represented by the ratio of the partial pressure divided by the saturation partial pressure, not the ppmv concentration.[11] Thus, low vapor pressure compounds can be detected at low vapor pressures by definition; with polymer sensors, it is seldom possible to detect below ∼0.1% of the saturation vapor pressure.[12] To make fair comparisons among all analytes for our studies here of analyte identification and selectivity, we have made all analyte concentrations at the same thermodynamic potential (i.e., saturation vapor pressure).

A detailed study is underway on LODs and LORs for colorimetric sensor arrays and will be reported elsewhere. Nonetheless, some sense of scale is possible from our current data. A listing of the saturation vapor pressures of the analytes examined is presented in Table 1. The array shows very good responsiveness to both Brønsted and Lewis bases and acids even with low vapor pressures, such as dibenzylamine (∼3 ppmv at 298 K), octanoic acid (∼49 ppmv), or octylthiol (∼0.1 ppmv). In previous work using more limited colorimetric sensor arrays, we have found LODs in the low ppbv range for amines, carboxylic acids, thiols, and phosphines.[2] The sensitivity of the array to bases and acids is a result of the strong metal−analyte interactions, either by metal ligation (i.e., coordination or dative bonding) or by Brønsted acid/

(10) Lide, D. H., Ed. *Handbook of Chemistry and Physics*; CRC Press: Ann Arbor, MI, 2004.

(11) Doleman, B. J.; Severin, E. J.; Lewis, N. S. *Proc. Natl. Acad. Sci. U.S.A.* **1998**, *95*, 5442−5447.

(12) A few reports of sub-ppmv measurements have appeared in the electronic nose literature: (a) Dickinson, T. A.; Michael, K. L.; Kauer, J. S.; Walt, D. R. *Anal. Chem.* **1999**, *71*, 2192−2198. (b) Schermer, H. V.; Corcoran, P.; James, M. K.; *Sens. Actuators, B* **1993**, *15−16*, 256. (c) Gardner, J. W.; Pearce, T. C.; Friel, S.; Bartlett, P. N.; Blair, N. *Sens. Actuators, B* **1994**, *18−19*, 240.

Table 1. Vapor Pressures at 298 K of 100 Common VOCs

analyte family	analyte	vapor pressure[a] (ppmv)	analyte family	analyte	vapor pressure[a] (ppmv)
alcohols	ethanol	78000	aromatic amines	pyridine	19700
	cyclopentanol	14000		2-picoline	14700
	3,3-dimethyl-2-butanol	9000		3-picoline	8000
	1-butanol	6300		4-picoline	7600
	3-hexanol	6300		3,5-lutidine	2300
	2-hexanol	3300		3,4-lutidine	1600
	1-pentanol	2200		aniline	660
	cyclohexanol	1300		3,5-dimethylaniline	170
	1-hexanol	1220		dibenzylamine	3
	2-phenyl-1-propanol	990	aromatics	benzene	133000
	phenol	360		toluene	36000
	2-octanol	320		*p*-xylene	11500
	cycloheptanol	270	carboxylic acids	trifluoroacetic acid	140000
	1-octanol	104		formic acid	43400
	benzyl alcohol	70		acetic acid	15000
	4-decanol	50		propionic acid	4900
	1-heptanol	38		2-chloropropionic acid	1400
	2-decanol	26		*tert*-pentanoic acid	990
	3-decanol	26		isobutyric acid	570
	1-nonanol	25		perfluorooctanoic acid	360
	1-decanol	11		pentanoic acid	300
	1-dodecanol	1.1		hexanoic acid	240
aldehydes	hexanal	14200		bromoacetic acid	160
	heptanal	5000		trichloroacetic acid	100
	octanal	2700		3-bromopropionic acid	100
	benzaldehyde	1270		chloroacetic acid	90
	nonanal	690		heptanoic acid	14
	o-tolualdehyde	410		octanoic acid	5
	(*d,l*)−2-phenylpropanal	380	esters	methyl octanoate	680
	1-myrtenal	190		methyl benzoate	440
	decanal	160		ethyl benzoate	230
aliphatic amines	triethylamine	92000		ethyl nonanoate	150
	di-*n*-propylamine	41500	hydrocarbons	1-octene	211000
	amylamine	39700		cyclohexene	113000
	di-*sec*-butylamine	10000		octane	14300
	diisobutylamine	9800		*trans*-5-decene	2630
	2-heptylamine	7600		1-decene	2600
	1,5-dimethylhexylamine	4200		dodecane	1320
	1-heptylamine	3900		tetradecane	48
	tert-octylamine	3800	ketones	3-heptonone	1840
	N,N-dimethylbenzylamine	2400		2-octanone	800
	di-*n*-butylamine	2300		3-decanone	350
	2-ethyl-1-hexylamine	1580	phosphines	dimethylphenylphosphine	1000
	1-octylamine	1280		tri-*n*-butylphosphine	90
	benzylamine	860	thiols	1-pentylthiol	18200
	cyclooctylamine	800		1-hexylthiol	5500
	N,N-dimethylhexylamine	770		cyclohexylthiol	5200
	1-nonylamine	360		benzylthiol	620
	1-decylamine	140		1-octylthiol	560
	1-undecylamine	56			
	dicyclohexylamine.	45			

[a] Vapor pressures from the EPA's EPI software suite (http://www.epa.gov/opptintr/exposure/docs/episuitedl.htm) or from Material Safety Data Sheets (MSDS); www.msdssearch.com. Due to differences among sources and small variations in temperatures, these values should be taken as approximate only.

base interactions. Weakly coordinating vapors such as esters, ketones, alcohols, arenes, and hydrocarbons show a lower response, just as the mammalian olfactory system does. In all likelihood, this is *not* coincidental, since many of the olfactory receptors probably contain a metal ion (e.g., Cu(II), Zn(II), and possibly Mn(II)) at their active site.[9] Since weakly coordinating, nonproton acidic or basic compounds are unable to interact strongly with most of our chromophores, their response is diminished. Even with hydrocarbons, however, the array can interact with vapors via van der Waals and solvatochromic interactions.

Chemometrics, Reproducibility, and Resolution. As discussed earlier, each analyte response is represented as the change in the red, green, and blue values of each of the 36 dyes, i.e., a 108-dimensional vector (the full digital data are available in the Supporting Information). To examine the multivariate distances between the analyte responses in this 108-dimensional RGB color space, a hierarchical cluster analysis (HCA) was performed using the usual minimum variance ("Ward's") method.[13] A hierarchical tree (i.e., dendrogram) of all 100 analytes is shown in Figure 7. For this HCA, the color differences were standardized in the usual fashion (i.e., (observed change − mean change)/(standard devia-
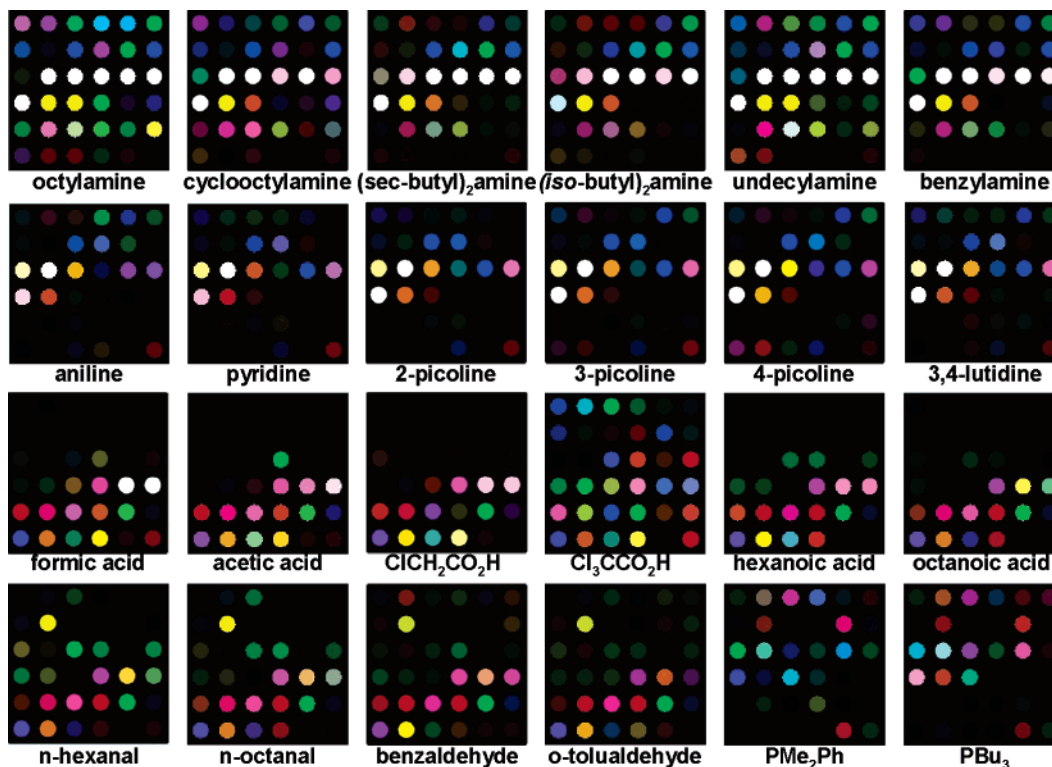
Figure 5. Colorimetric array response to VOCs visualized as color difference maps. Shown are 24 representative VOCs after equilibration at their vapor pressure at 295 K. Full digital data for 100 VOCs are provided in the Supporting Information. The color range of these difference maps are expanded from 6 to 8 bits per color (RGB range of 4–67 expanded to 0–255).
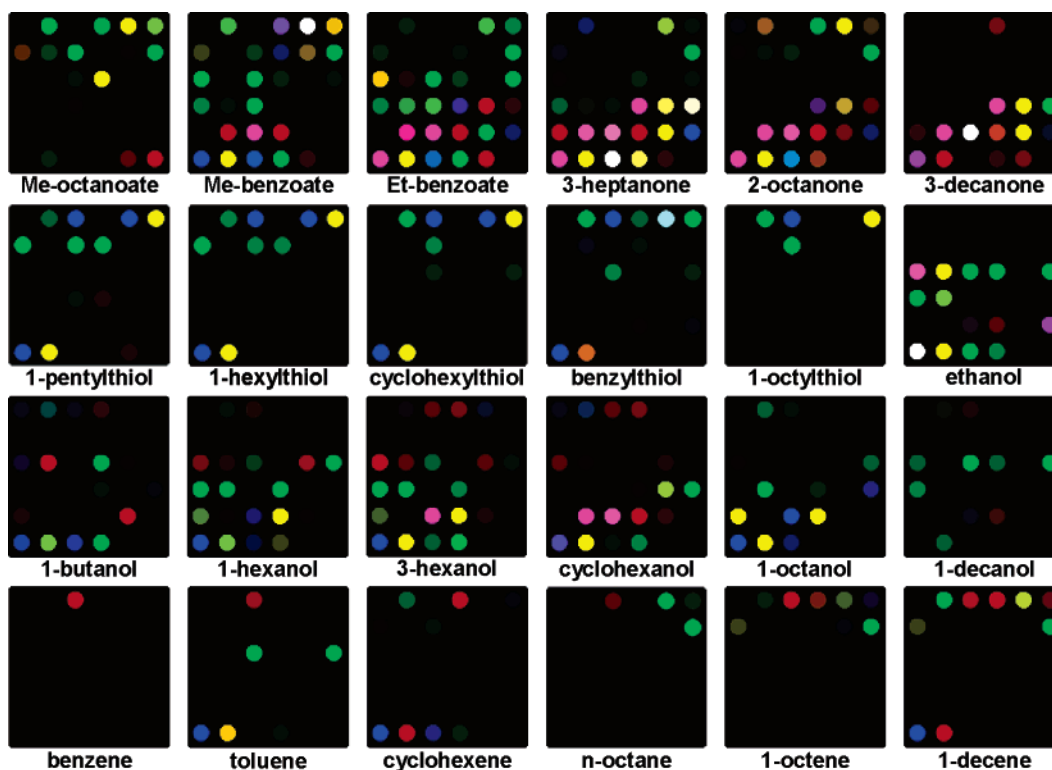

Figure 6. Colorimetric array response for 24 representatives of less responsive organic compounds at their vapor pressure at 295 K; color range expanded from 4 to 8 bits per color (8–17 expanded to 0–255).

tion) for each dye) so as to weight all dyes equally.

An advantage of array-based chemical sensing is that it can respond to analytes for which it was not originally designed to detect: in principle, even for an unknown compound, a sensor array should be able to tell us what the unknown is *like*. The vectors representing the analytes cluster according to the functional group of the organic compound: aromatic amines, aliphatic amines, carboxylic acids, strong acids, aldehydes, thiols, and
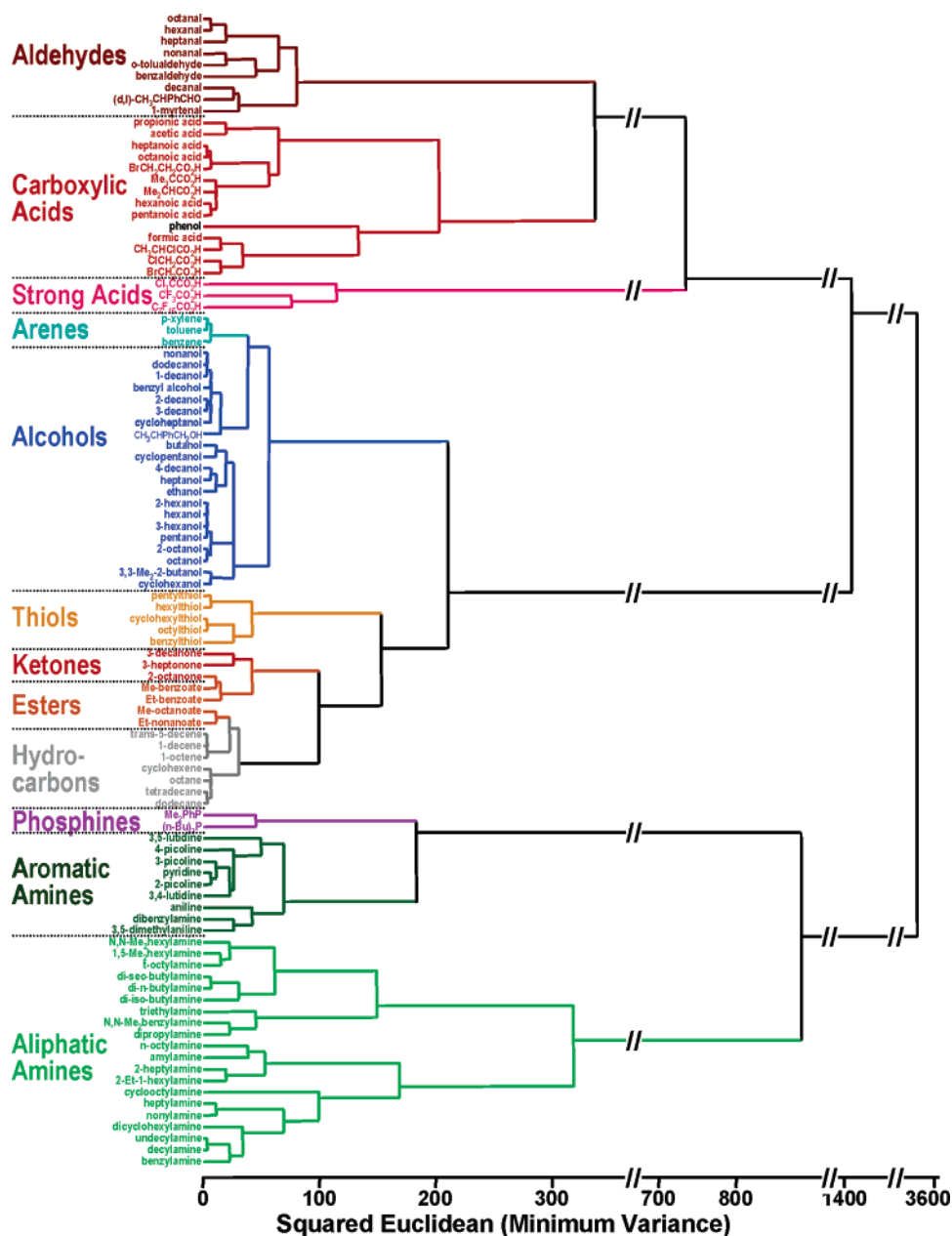
Figure 7. Dendrogram of the colorimetric array responses to 100 common VOCs at full vapor pressure at 295 K. Averages of three trials were used for each analyte.

phosphines form distinct branches in the hierarchical tree. Alcohols, ketones, esters, and even arenes and hydrocarbons (alkanes and alkenes) form separate clusters, despite the relatively weak response of the array to these chemical classes. The important lesson from the HCA is that once a library of array responses is created, the *chemical class* of new analytes can be readily identified. Among all 100 compounds, only one, phenol, was classed "incorrectly", finding itself among the carboxylic acids; given phenol's unusually high acidity, however, it is probably more accurate to consider it an "honorary" carboxylic acid than an alcohol. As discussed elsewhere in greater detail with more examples, very fine distinctions within individual chemical classes

can be easily made, especially if one includes bis-pocketed porphyrins[14] to probe the steric demands of analytes:[2e] linear alkylamines are discernible from cyclic amines, primary from secondary from tertiary, alkyl from aromatic, etc.

The complete database (available in the Supporting Information) consists of the 108-dimensional vectors that are the change in RGB values for each of the triplicate runs for each of the 100 analytes plus an average response for each analyte. Triplicate data were acquired to probe the reproducibility of the array response to each analyte. The unweighted Euclidean distance between any

(13) (a) Beebe, K. R.; Pell, R. J.; Seasholtz, M. B. *Chemometrics: Practical Guide*; J. Wiley & Sons: New York, 1998. (b) Haswell, S. J., Ed. *Practical Guide to Chemometrics*; Marcel Dekker: New York, 1992.

(14) (a) Sen, A.; Suslick, K. S. *J. Am. Chem. Soc.* **2000**, *122*, 11565. (b) Suslick, K. S. In *The Porphyrin Handbook*; Kadish, K., Smith, K., Guilard, R., Eds.; Academic Press: New York, 2000; Vol. 4, Chapter 28, pp 41−63. (c) Bhyrappa, P.; Vaijayanthimala, G.; Suslick, K. S. *J. Am. Chem. Soc.* **1999**, *121*, 262−263. (d) Bhyrappa, P.; Young, J. K.; Moore, J. S.; Suslick, K. S. *J. Am. Chem. Soc.* **1996**, *118*, 5708−5711.
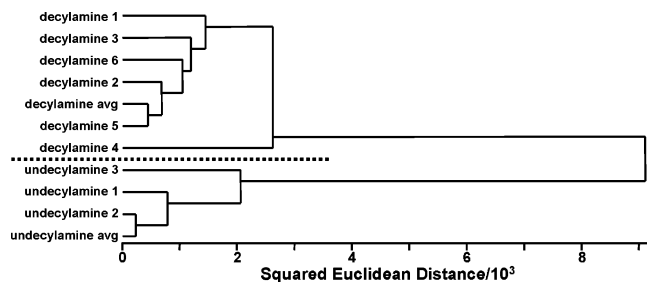
Figure 8. HCA dendrogram showing the response reproducibility and facile differentiation among 9 different printed arrays exposed to decylamine ($C_{10}H_{21}NH_2$) compared to undecylamine ($C_{11}H_{23}NH_2$); saturated vapor pressure at 295 K.

two entries is a useful measure of their similarity: entries for separate array exposures to the same analyte should be closer to each other than to any other analyte's entries. To probe the accuracy of analyte recognition by the colorimetric sensor arrays, the entire database was queried against itself. Every entry of the database was compared against every other entry by determining the unweighted Euclidean distance between them (Supporting Information). For every pair of closest entries, both entries always were for the same analyte: i.e., there were *no misidentifications out of the entire 400-entry database*. The error rate therefore is <0.25%.

The reproducibility of response of the colorimetric sensor array was tested, and the results are shown in Figure 8. A detailed comparison of *n*-decylamine ($C_{10}H_{21}NH_2$) to *n*-undecylamine ($C_{11}H_{23}NH_2$) was undertaken to determine reproducibility of the response of the arrays; these analytes were used for this test because they have extremely similar array responses, relative to the whole library (cf. Figure 7). For data taken on nine separate arrays (printed separately on different dates, in different batches), as seen in Figure 8, the Euclidean distances between the decylamine and undecylamine classes in the HCA are well resolved. Even the largest spread for decylamine (trial 4 vs rest of cluster), for example, is less than a third of the distance between the decylamine and undecylamine clusters. In a separate set of trials of 11 runs of *n*-decylamine, the average squared Euclidean distance (SED) between pairs of analyses was 2087 (ranging from 689 to 3985), whereas the SED between decylamine and undecylamine clusters was 9076.

The greatest remaining source of variability with the arrays lies in the quality of their printing. The arrays are currently printed manually using an array of slotted pins, as has often been used for DNA array printing. It is anticipated that use of a robotic noncontact printer will lead to still better print quality and further enhanced array reproducibility. Work toward this goal is currently in progress.

Fortunately, by using the *change* in color values of the array before and after exposure to the analyte, much of the variation in printing from array to array is canceled out. We can show this quantitatively using the Kubelka–Munk (KB) theory.[15] In its simplest approximate form, the KB equation is

$$(1 - R)^2 / 2R = \epsilon C / S \qquad (1)$$

where R is the reflectance (i.e., roughly the RGB values from the scanner expressed as a fraction from 0 (no reflectance) to 1 (total reflectance)), ϵ is the extinction coefficient of the dye, C is the concentration of the dye, and S is a scattering coefficient dependent upon the solid on which the dye is immobilized. As shown in Figure 9a and b, the observed changes in color values of dye spots are well represented by the KB equation. We then use this equation to model a calculated color difference as a function of dye concentration: Figure 9c shows an example for model data at a single wavelength for a dye spot, where the ratio of the effective extinction coefficient is 0.5 for the dye before versus the dye after analyte exposure. Note that, as the dye concentration increases, the color value *change* approaches a constant; i.e., errors in dye concentration during printing cancel for highly colored spots. In the specific case illustrated, if initial dye spot color value is ~150, then the color value change (i.e., ΔR, ΔG or ΔB) is ~30 (both values are roughly typical of dyes in the colorimetric sensor array). In this case, a 15% change in concentration (or amount of dye deposited), for example, leads to only a 5% change in the observed R, G, or B color value, and only a 0.6% difference in the color value change in R, G, or B.

Principal Component Analysis. Principal component analysis (PCA)[13] can be used to determine the number of meaningful independent dimensions probed by a cross-reactive array. The eigenvector of each principal component defines the linear combination of the response of each sensor parameter by the amount of variance in the data along each principal component. The total number of independent eigenvectors must be $n - 1$ for n-dimensional data for a sufficiently large data set (i.e., one containing at least n number of analytes). Even for diverse libraries of VOCs, PCA for most prior electronic nose technology is dominated by only two or three independent dimensions; in fact, there is often a *single* dominant dimension that accounts for *>90% of the total discrimination* and roughly corresponds to sensor hydrophobicity. This very limited dimensionality (or "dispersion") means that very little of the total diversity of chemical properties is being probed in traditional electronic nose technology: this is the inherent result of relying primarily on van der Waals interactions (e.g., adsorption to metal oxide surfaces or sorption onto or into polymer films) for molecular recognition.

Because of the limited dispersion in past sensor arrays, the data obtained with traditional electronic nose technologies is typically plotted against the two most important PCA dimensions. For showing differences between analytes, this approach can work *only because the dimensionality of the PCA is extremely limited.* If one is using an array of cross-reactive sensors, and PCA can reduce the response of the array to only two or three dimensions, one may well ask what the whole point of an array was in the first place! If an array of sensors can be reduced to simply two dimensions, then in principle, two properly chosen sensors are all that is necessary for the same resolution.

The colorimetric sensor array, in contrast, is not limited to van der Waals interactions but rather employs a variety of intermolecular interactions between the dyes and the analytes. The numerous and diverse interactions explore a broad area of chemical properties space. This diverse set of interactions spreads

(15) (a) Kubelka P.; Munk F. *Z. Tech. Phys.* **1931**, *12*, 593–601. (b) Kuehni, R. G. *Color, An Introduction to Practice and Principles*; Wiley: New York, 1997; Chapter 8. (c) Molenaar, R.; ten Bosch, J. J.; Zijp, R. J. *Appl. Opt.* **1999**, *38*, 2068–2077.
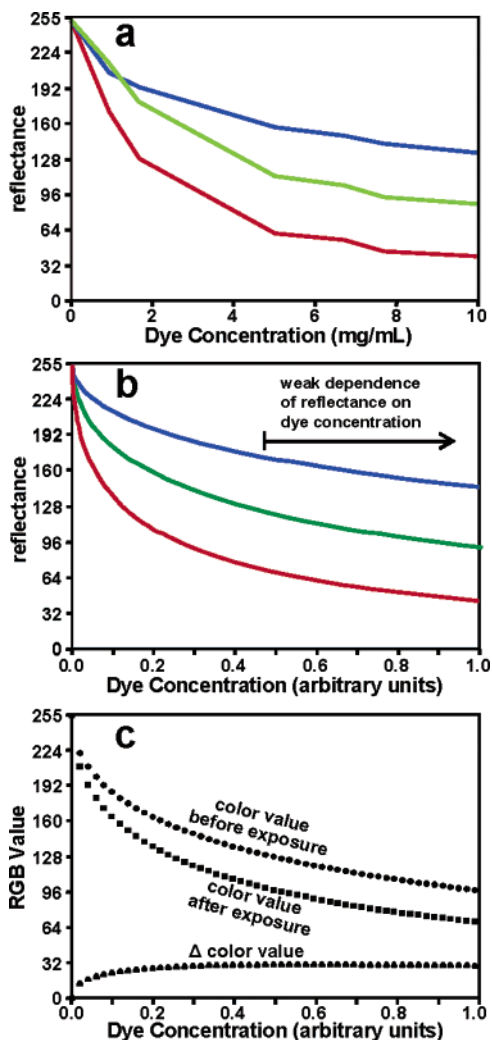
Figure 9. Kubelka–Munk model of reflectance and error cancellation by differencing. (a) Observed RGB color values of a spot of cresol red dye as a function of dye concentration in the spotting solution. (b) Kubelka–Munk model of the data. (c) Calculated color difference vs dye concentration, using the Kubelka–Munk equation and model data at a single wavelength for a dye spot, where the ratio of the effective extinction coefficient is 0.5 for the dye before vs the dye after analyte exposure. Note that as the dye concentration increases, the color value change approaches a constant, i.e., errors in dye concentration during printing cancel for highly colored spots.

the variation among the database entries (i.e., the discrimination among VOCs) over many independent dimensions (i.e., eigenvectors). As shown in Figure 10, PCA of the averaged responses to 100 VOCs shows that 90% of the discriminatory range requires 14 dimensions, 95% of total discrimination requires 22 dimensions, and 99% requires 40 dimensions (out of a possible 99 independent dimensions, i.e., $n - 1$, where n is the number of analytes in database; for an unlimited sized data set, our 6×6 array has a total possible 108 dimensions, i.e., red, green, and blue color changes for 36 dyes). By probing a much wider range of chemical interactions, we have dramatically increased the dispersion of our sensor array. It is this increased dimensionality that permits us to discriminate among very closely related analytes, e.g., decylamine versus undecylamine, as discussed earlier.

If we take the colorimetric array responses and reduce the dimensionality of the data to two dimensions, only 53% of the
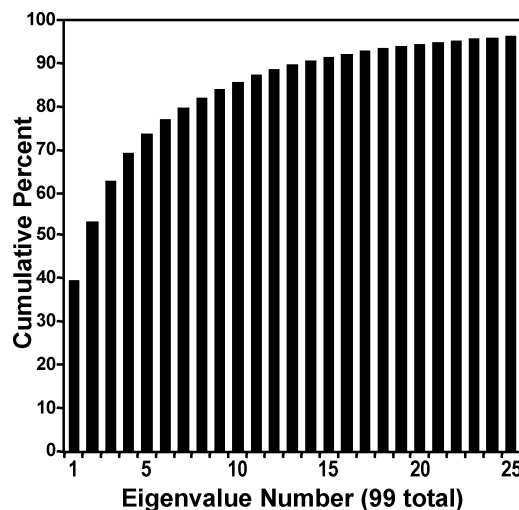

Figure 10. PCA from 100 VOCs showing that our colorimetric sensor array has an extraordinarily high level of dispersion. Fourteen dimensions are required to define 90% of the total variance, 22 dimensions for 95% of the total variance, and 40 dimensions for 99%.
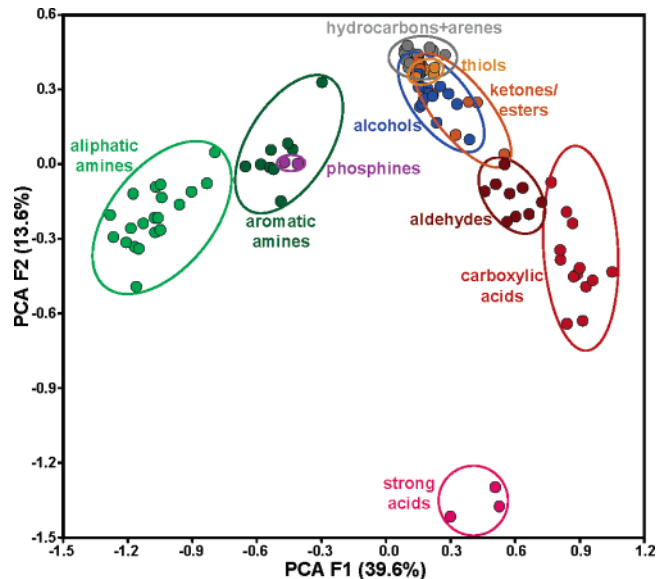

Figure 11. Two principal components of the colorimetric sensor array from the response data averages of the 100 VOCs at 295 K, at their full vapor pressure. Only 53% of the total discriminatory separation is captured by these first two components, so only fair spatial discrimination among chemical classes (shown in the same color scheme as Figure 7) can result. When the full dimensionality of the array response is used (i.e., by HCA as in Figure 7), there are no confusions among analyte classes or between closely related analytes.

discriminatory ability of the array is captured, as shown in Figure 11. As an inherent consequence, the separation of analytes into their chemical classes is limited. Significant overlap of the hydrocarbons, thiols, ketones, esters, and aldehydes is observed, and phosphines cannot be distinguished from aromatic amines. This is *not* a negative reflection on the colorimetric array, but rather it emphasizes how poor the dispersion of past technologies has been. As shown using the full dimensionality of the array in a hierarchical cluster analysis, the colorimetric sensor array is capable of chemical classification essentially without error among the 100 VOCs in the library examined and can distinguish even very closely related analytes without difficulty.

One of the most important applications of a sensor array is that it should easily produce a unique response to complex mixtures (coffees, perfumes, etc.) without the need for the mixture to be broken down into its component parts. Such fingerprinting, however, requires a very high dimensionality of the principal components such as that present with our array. The number of possible differentiable patterns available to the colorimetric array is immensely large, as we will illustrate through the following "back-of-the-envelope" calculation. In principle, each of the 108 dimensions in the possible color differences of the 36-dye array can take on 1 of 511 possible values (the range is -255 to $+255$), for inexpensive 8-bit scanners or digital cameras. The maximum number of possible patterns is then $(511)^{108}$. In practice, RGB color change values do not range over the full 511 possible values; the color change values, however, are still substantial. For example, the maximum observed change in the database of 100 VOCs is -205 and the first 300 largest absolute values of color changes are all >100; for any given analyte, however, most dyes do not change color much at all, and so the overall mean of the absolute values of the color changes is only 16.4. We will make the extremely conservative estimate of the average color change being 16.4 per dimension (a gross underestimate, because the important PCA dimensions are dominated by the more highly responsive dyes). A difference of 4 in the R, G, or B values is adequate to detect a change (also a large overestimate), and then our resolution per dimension is 4.1. From the principal component analysis, 95% of all information is contained in 22 specific dimensions (i.e., linear combinations of the 108 different R, G, and B values). This implies a conservative lower limit of discrimination that is still huge: $(16.4/4)^{22} = 3 \times 10^{13}$ distinctly recognizable patterns for a 36-dye colorimetric sensor array. While we realize that there are hidden assumptions and gross simplifications in this rough analysis, it does show the critical importance that high dimensionality has for the success any electronic nose technology.

CONCLUSION

The colorimetric sensor array represents a fundamental new approach to array-based chemical sensing. Based on a broad range of chemical-sensing interactions, rather than on weak nonspecific van der Waals forces, the disposable array exhibits both excellent sensitivity and selectivity to a broad range of organic compounds.

The array is particularly well-suited for the detection of biogenically important analytes, such as amines, thiols, and acids. In contrast to nearly all prior electronic nose technologies, data from the colorimetric sensor array is highly dispersed among many independent dimensions: i.e., 95% of the discriminatory range requires 22 independent dimensions. The arrays are essentially nonresponsive to changes in humidity, which avoids the common problem of interference from changes in humidity during real-world analyses. The array shows very good responsiveness to both Brønsted and Lewis bases and acids even with low vapor pressures. We have found (in previous work using more limited colorimetric sensor arrays) LODs in the low ppbv range for amines, carboxylic acids, thiols, and phosphines.[2] The sensitivity of the array to bases and acids is a result of the strong metal−analyte interactions, either by metal ligation (i.e., coordination or dative bonding) or by Brønsted acid/base interactions. Weakly coordinating vapors such as esters, ketones, alcohols, arenes, and hydrocarbons show a lower response, just as the mammalian olfactory system.

SUPPORTING INFORMATION AVAILABLE

Array response and chemometric data. This material is available free of charge via the Internet at http://pubs.acs.org.